Three-Dimensional Axisymmetric Stagnation-Point Flow in a Nanofluid with Nanoparticles via Moving Surface

Jyothi S.[1], Suresh Babu R.[2*], Aravind H. R.[3], Ashfar Ahmed[4], G. Tamilarasi[5*], Motamari Madhu[6]

[1]Department of Mathematics, Mangalore Institute of Technology & Engineering, Moodabidre-574227, Karnataka, India

[2]Department of Mathematics, M S Ramaiah Institute of Technology, Bangalore-560054, Karnataka, India

[3] Department of Mathematics, Cambridge Institute of Technology, Bengalore-560036, Karnataka, India

[4] Department of Mathematics, Malla Reddy Engineering College (Autonomous), Main Campus, Maisammaguda, Medical, Secundrabad-500100, Telangana, India

[5]Department of Mathematics, Kalasalingam Academy of Research and Education, Krishnankoil, Virudhunagar-626126, Tamilnadu, India

[6]Department of Mathematics, University College, Palamuru University, Mahabubnagar-509001, Telangana, India

*Corresponding Author: tamiltara5@gmail.com, sureshbabur@msrit.edu

Abstract

In this paper unsteady three-dimensional axisymmetric stagnation point and convection boundary layer flow of nanofluid over a moving surface with anisotropic slip is examined different thermal and concentration boundary layer fraction. The numerical model of nanofluid has been used. The Navier-Stokes and heat equation state numerical solutions. The problem is reduced by a set of appropriate similarity transformations, the basic coupled nonlinear partial differential equations into the ordinary differential equations. The translating resulting equations are solved numerically by using shooting technique with Runge-Kutta-Fehlberg fourth order method in MATLAB. We found that the influence of different physical parameters on temperature, concentration profiles as well as heat transfer rate.

Key Words: Axisymmetric, Stagnation Point Flow, Nanofluid, Nanoparticles, Moving Surface.

Introduction:

The study of SP motion and HT via SS has garnered significant attention from researchers due to its broad range of industrial and engineering applications. These include processes such as rapid spray cooling and quenching in metal foundries, emergency core cooling systems, microelectronics cooling, and ice chillers in air conditioning. Other areas of application include wire drawing, polymer extrusion, continuous metal casting, adhesive tape production, and glass blowing. For example, spray cooling is a highly efficient method for removing high heat flux from heated sheet surfaces through convection. Narisimha Reddy et al. [1] focused on the Casson NFs motions in industry via a non-linear SS. The effect of IMF (Induced magnetic field) on liquid motion close to standstill point created via SS by developed Khan et al. [2]. Mahmood et al. [3] proposed the steady SP motion with viscous dissipation via a Permeable SS. Vinodkumar et al. [4] consider the MHD SP motion of Williamson HNFs with CR and energy generation effects via porous extending sheet. The MHD bioconvective micropolar NFs motion with migrating microorganisms via vertically extending material was analysed by Fatunmbi et al. **[5]**. Boujelbene et al. **[6]** examined the numerical analysis of 3D radiative, steady viscoelastic NFs motion via exponentially SPS. Jawad et al. **[7]** illustrate the ratification of chemically reactive tangent hyperbolic fluid owing to bidirectional SS. Li et al. **[8]** focused the effect associated with mass and heat transport in a liquid motion with heat source or sink. Fatima et al. **[9]** illustrate the theoretical model could be applied to engineering methods, heat transfer and thermal energy.

Heat generation in nanofluid motion refers to the internal production of heat within a nanofluid as it flows, which can significantly affect its thermal behavior. Nanofluids, which are fluids with nanoparticles dispersed in them, typically exhibit enhanced thermal conductivity and heat transfer capabilities. However, when there is internal heat generation, such as due to chemical reactions, viscous dissipation, or external sources like electromagnetic fields, it alters the temperature distribution within the fluid. This added heat can influence the nanofluid's flow characteristics, potentially causing variations in velocity, viscosity, and thermal gradients. Understanding heat generation in nanofluid motion is essential for optimizing thermal systems, such as cooling technologies, microelectronics, and energy devices, where efficient heat management is crucial. Sun et al. [10] perform to numerical boundary layer motion via plate in porous medium filled with bioconvection nanofluid with motile gyrotactic microorganisms. Hussain et al. [11] presented the bioconvection technology is measured as a necessary procedure with suppressed compensation in bio-fuel. Dharmaiah et al. [12] presented the thermal efficiency of heat transfer phenomena is considerably improved when nanoparticles are combined. The influence of mass and heat transfer on MHD bioconvective peristaltic transport of Powell-Eyring nanofluid via a curved surface was examined by Iqbal et al. [13]. Naveed Khan et al. [14] described the numerical analysis of MHD bioconvective base Casson HNF motion via vertical cone. Ahmed et al. [15] explored the bioconvection motion of Casson NFs by a rotating disk with impact of Joule heating and heat source. Th heat generation effect on mixture base HNFs with bioconvection effect via linear convectively heated SS was focused by Hussain et al. [16]. Farooq and Tao [17] described the MHD bioconvective NFs with varying viscosity via non-similarity analysis. Abbas and Khan et al. [18] explained the MHD motion of cross NFs with gyrotactic microorganisms and thermophoretic particle deposition via sheet. Arafa et al. [19] presented bioconvective Bödewadt motion of NFs via 3D stretched rotating disk. Ullah et al. [20] described the characteristics of heat generation and absorption in a 3D mixed bioconvection motion of Casson NFs via stretching cylinder.

A bioconvection nanofluid with microorganisms is a complex fluid system where motile microorganisms, such as bacteria or algae, interact with nanoparticles suspended in a base fluid. The microorganisms' collective movement, driven by stimuli like light (phototaxis) or chemical gradients (chemotaxis), creates self-organized convective currents known as bioconvection. These currents, combined with the enhanced thermal conductivity and mass transport properties of the nanofluid, improve overall heat and mass transfer. This system has applications in areas like advanced cooling technologies, bio-microfluidics, and bioreactor optimization, leveraging the unique properties of both microorganisms and nanoparticles for enhanced performance. Puneeth et al. [21] examines the motion of Ree-Eyring nanofluid via SS. Kumar Sarma et al. [22] explored the 2D MHD Darcy Forchheimer Casson fluid flow via SS. Khan et al. [23] described the bioconvection phenomena with gyrotactic microorganisms and micropolar nanofluid model with hydro magnetic flow. Farooq et al. [24] investigate characteristics of bioconvective MHD motion via extending porous surface. Farooq et al. [25] presented the MHD bioconvective micropolar nanofluid with Soret and Dufour effects bynon-similarity analysis.

Formulation of the problem

We considered the effect of AS on the 3D motion of microorganisms at a SP on a moving surface with heat generation and CR. Some of the considerations in the current work are as follows:

1. The Cartesian coordinate system x_1, y_1 and z_1 with the corresponding motion velocities u^*, v^* and s^* is presented in Figure 1.
2. Assume that the x_1 - direction is aligned via striations of plate, y_1 - direction is normal to striation and z_1 - direction is stagnation liquid motion direction.
3. The velocity $\left(U^*, V^*, 0\right)$ of the plate is constant, where the components U^* and V^* are in x_1 and y_1 - directions, respectively.
4. Potential flow propels the liquid at a distance from the plate is $u^* = a_1 x_1, v^* = a_1 y_1$ and $s^* = -2 a_1 z_1$, where a_1 is the strength of the stagnation motion.
5. The uniform temperature, nanoparticle volume fraction and concentration of microorganisms at the plate and far from the plate are g $T_{w,}$ C_w, *and* N_w and T_∞, C_∞ and N_∞ respectively.
6. Based on the physical liquid motion model, we can form the field equations as follow

$$\nabla . V = 0 \tag{1}$$

$$\rho_f (\mathrm{V}.\nabla).\mathrm{V} = -\nabla \mathrm{p} + \mu \nabla^2 \mathrm{V} \tag{2}$$

$$\frac{\partial T}{\partial t} + \mathrm{V}.\nabla T = \alpha_m \nabla^2 T + \tau \left\{ D_B \nabla T . \nabla C + \left(D_T \big/ T_\infty \right) \nabla T . \nabla T \right\} \tag{3}$$

$$\frac{\partial C}{\partial t} + \left(\mathrm{V}.\nabla \right) C = D_B \nabla^2 C + \left(D_T / T_\infty \right) \nabla^2 T - K_0 \left(C - C_\infty \right) \tag{4}$$

Equations (2)-(4) can be formed as

$$\frac{\partial u^*}{\partial x_1} + \frac{\partial v^*}{\partial y_1} + \frac{\partial s^*}{\partial z_1} = 0 \tag{5}$$

$$u^* \frac{\partial u^*}{\partial x_1} + v^* \frac{\partial u^*}{\partial y_1} + s^* \frac{\partial u^*}{\partial z_1} = -\frac{1}{\rho_f} \frac{\partial p^*}{\partial x_1} + \upsilon \left(\frac{\partial^2 u^*}{\partial {x_1}^2} + \frac{\partial^2 u^*}{\partial {y_1}^2} + \frac{\partial^2 u^*}{\partial {z_1}^2} \right) \tag{6}$$

$$u^* \frac{\partial v^*}{\partial x_1} + v^* \frac{\partial v^*}{\partial y_1} + s^* \frac{\partial v^*}{\partial z_1} = -\frac{1}{\rho_f} \frac{\partial p^*}{\partial y_1} + \upsilon^* \left(\frac{\partial^2 v^*}{\partial {x_1}^2} + \frac{\partial^2 v^*}{\partial {y_1}^2} + \frac{\partial^2 v^*}{\partial {z_1}^2} \right) \tag{7}$$

$$u^* \frac{\partial s^*}{\partial x_1} + v^* \frac{\partial s^*}{\partial y_1} + s^* \frac{\partial s^*}{\partial z_1} = -\frac{1}{\rho_f} \frac{\partial p^*}{\partial z_1} + \upsilon^* \left(\frac{\partial^2 s^*}{\partial {z_1}^2} + \frac{\partial^2 s^*}{\partial {y_1}^2} + \frac{\partial^2 s^*}{\partial {z_1}^2} \right) \tag{8}$$

$$\left. \begin{aligned} u^* \frac{\partial T_1}{\partial x_1} + v^* \frac{\partial T_1}{\partial y_1} + s^* \frac{\partial T_1}{\partial z_1} = \alpha_1 \left(\frac{\partial^2 T_1}{\partial {x_1}^2} + \frac{\partial^2 T_1}{\partial {y_1}^2} + \frac{\partial^2 T_1}{\partial {z_1}^2} \right) + \tau^* D_B \left(\frac{\partial C_1}{\partial x_1} \frac{\partial T_1}{\partial x_1} + \frac{\partial C_1}{\partial y_1} \frac{\partial T_1}{\partial y_1} + \frac{\partial C_1}{\partial z_1} \frac{\partial T_1}{\partial z_1} \right) \\ + \frac{\tau^* D_{T_1}}{T_\infty} \left(\left(\frac{\partial T_1}{\partial x_1} \right)^2 + \left(\frac{\partial T_1}{\partial y_1} \right)^2 + \left(\frac{\partial T_1}{\partial z_1} \right)^2 \right) + \frac{Q_0}{\rho_f} \left(T - T_\infty \right) \end{aligned} \right\} \tag{9}$$

$$u^* \frac{\partial C_1}{\partial x_1} + v^* \frac{\partial C_1}{\partial y_1} + s^* \frac{\partial C_1}{\partial z_1} = D_B \left(\frac{\partial^2 C_1}{\partial {x_1}^2} + \frac{\partial^2 C_1}{\partial {y_1}^2} + \frac{\partial^2 C_1}{\partial {z_1}^2} \right) + \frac{D_{T_1}}{T_\infty} \left(\frac{\partial^2 T_1}{\partial {x_1}^2} + \frac{\partial^2 T_1}{\partial {y_1}^2} + \frac{\partial^2 T_1}{\partial {z_1}^2} \right) - K_1 \left(C - C_\infty \right) \tag{10}$$

Consider the equations (8)-(13) of Gov. Eq's, which are subjected to the AS on a moving surface sheet.
The variables of interest are the NPs volume fraction and the surface temperature. The given conditions are as follows:

$$\left. \begin{aligned} & u^* - U_1 = N_2 \mu^* \frac{\partial u^*}{\partial z_1} \quad v^* - V_1 = N_3 \mu^* \frac{\partial v^*}{\partial z_1} \quad s^* = 0 \quad -k^* \frac{\partial T_1}{\partial z_1} = \mathrm{h}_f (\mathrm{T}_f - \mathrm{T}_1) \\ & \qquad D_B \frac{\partial C_1}{\partial z_1} + \frac{D_{T_1}}{T_\infty} \frac{\partial T_1}{\partial z_1} = 0 \;\; N_1 = N_w : \qquad at \quad z_1 = 0 \\ & u^* = a_1 x_1 \;\; v^* = a_1 y_1 \;\; s^* = -2 a_1 z_1 \;\; T_1 = T_\infty \;\; C_1 = C_\infty \;\; N =_1 0 \quad at \quad z_1 = \infty \end{aligned} \right\} \tag{11}$$

We are looking for a solution to the steady state equations (8)-(10). Recently, the Bernoulli equation for an inviscid fluid, where the fluid is assumed to be non-viscous outside of the BL, has been used.

$$\frac{p^*}{\rho_f} + \frac{1}{2} \left| v^* \right|^2 = cons\,\mathrm{tant} \tag{12}$$

Using equations (15) & (16), we have

$$-\frac{1}{\rho_f} \frac{\partial p^*}{\partial z_1} = 0 \tag{13}$$

$$\frac{p^*}{\rho_f}+\frac{1}{2}\left(\left(u^*\right)^2+\left(v^*\right)^2+\left(w^*\right)^2\right)=cons\tan t \tag{14}$$

$$\frac{p^*}{\rho_f}+\frac{1}{2}\left(a_1{}^2\left(u^*\right)^2+a_1{}^2\left(v^*\right)^2+4a_1{}^2\left(w^*\right)^2\right)=cons\tan t \tag{15}$$

At $z_1=0,\ w^*=0$

$$\frac{p^*}{\rho_f}+\frac{1}{2}a_1{}^2\left(x_1{}^2+y_1{}^2\right)=cons\tan t \tag{16}$$

At $(x_1, y_1, z_1)=(0,0,0),\ p^*=p_0$

$$p^* = p_0-\frac{1}{2}\rho_f a_1{}^2\left(x_1{}^2+y_1{}^2\right) \tag{17}$$

where stagnation pressure p_0

The B.C.'s Eq. (11) suggests that the equations (8)-(10) have similarity transformations of the following forms.

$$\begin{gathered} u^*=a_1 x_1 f'(\eta)+U_1 h(\eta) \quad v^*=a_1 y_1 g'(\eta)+V_1 k(\eta) \quad s^*=-\sqrt{a_1\upsilon^*}\left(f(\eta)+g(\eta)\right) \\ \eta=\sqrt{\frac{a_1}{\upsilon^*}}z \quad \theta(\eta)=\frac{T_1-T_\infty}{T_w-T_\infty} \quad \phi(\eta)=\frac{C_1-C_\infty}{C_w-C_\infty} \quad w(\eta)=\frac{N_1}{N_w} \end{gathered} \tag{18}$$

With the help of the above equations (18), the equations (8)-(10) are converted into the following ordinary differential equations (ODEs):

$$f'''=-(f+g)f''+(f')^2-1 \tag{19}$$

$$h''-(f+g)h'+hf' \tag{20}$$

$$g'''=-(f+g)g''+(g')^2-1 \tag{21}$$

$$k''=-(f+g)k'+kg' \tag{22}$$

$$\theta''=-\Pr(f+g)\theta'-N_b\theta'\phi'-N_t\left(\theta'\right)^2 \tag{23}$$

$$\phi''=-\Pr Le(f+g)\phi'-\frac{N_t}{N_b}\theta'' \tag{24}$$

$$w''=-Sc(f+g)w'+Pe(w'\phi'+w\phi'') \tag{25}$$

The equation (11) of B. C is subject to the following conditions:

$$\left.\begin{array}{l} f(0)=0 \quad f'(0)=\lambda_1 f''(0) \quad g(0)=0 \\ g'(0)=\lambda_2 g''(0),\quad h(0)-1=\lambda_1 h'(0) \\ k(0)-1=\lambda_2 k'(0),\quad \theta'(0)=-\gamma(1-\theta(0)) \\ N_b\phi'(0)+N_t\theta'(0)=0 \quad w(0)=1 \\ f'(\infty)=1 \quad g'(\infty)=1 \quad h(\infty)=0 \\ k(\infty)=0,\quad \theta(\infty)=0 \quad \phi(\infty)=0 \quad w(\infty)=0 \end{array}\right\} \tag{16}$$

In this work, several physically important quantities are considered. These include the local Nusselt number in the x-direction, the LNN in the y-direction, the skin friction, the mass flux, and the density flux of the motile microorganisms. Mathematically, we have

$$\left.\begin{aligned} &Nu_x = \frac{xq_w}{k(\mathrm{T}_w - \mathrm{T}_\infty)} \quad C_{fx} = \frac{\tau_{wx}}{\rho_f U^2} \quad Q_{mx} = \frac{xq_m}{D_B(\mathrm{C}_w - \mathrm{C}_\infty)} \quad Q_{nx} = \frac{xq_m}{D_n(\mathrm{N}_w - N_\infty)} \\ &\mathrm{Nu}_y = \frac{yq_w}{k(\mathrm{T}_w - \mathrm{T}_\infty)} \quad C_{fy} = \frac{\tau_{wy}}{\rho_f V^2} \quad Q_{my} = \frac{yq_m}{D_B(\mathrm{C}_w - \mathrm{C}_\infty)} \quad Q_{ny} = \frac{yq_m}{D_n(\mathrm{N}_w - N_\infty)} \end{aligned}\right\} \tag{17}$$

where $\tau_{wx} = \mu^* \left(\frac{\partial u^*}{\partial z_1}\right)_{z_1=0}$ $\tau_{wy} = \mu^* \left(\frac{\partial v^*}{\partial z_1}\right)_{z_1=0}$ $q_m = -k^* \left(\frac{\partial T_1}{\partial z_1}\right)_{z_1=0}$ $\mathrm{q}_m = -D_B \left(\frac{\partial C_1}{\partial z_1}\right)_{z_1=0}$ $q_m = -D_n \left(\frac{\partial N_1}{\partial z_1}\right)_{z_1=0}$

Substituting eq's (22) and (31) into eq. (32), we get

$$\left.\begin{aligned} &\mathrm{Re}_x^{-1/2} Nu_x = \mathrm{Re}_y^{-1/2} Nu_y = -\theta'(0) \qquad \mathrm{Re}_x^{-1/2} C_{fx} = \left(\frac{x}{L}\right)^2 f''(0) + \left(\frac{x_1}{L}\right) h'(0) \\ &\mathrm{Re}_y^{-1/2} C_{fy} = \left(\frac{x_1}{L}\right)^2 \mathrm{g}''(0) + \left(\frac{x_1}{L}\right) \mathrm{k}'(0) \quad \mathrm{Re}_x^{-1/2} Q_{mx} = \mathrm{Re}_y^{-1/2} Q_{my} = -\frac{\phi'(0)}{\phi(0)} \\ &\mathrm{Re}_x^{-1/2} Q_{nx} = \mathrm{Re}_y^{-1/2} Q_{ny} = -W'(0) \end{aligned}\right\} \tag{18}$$

where $\mathrm{Re}_x = a_1 x_1^2 / v^*$ *and* $\mathrm{Re}_y = a_1 y_1^2 / v^*$ are the local Reynolds numbers along x_1 and y_1 - directions.

Results and Discussion:

The impact of λ_1 (Slip Factor) $\theta(\eta)$ as predicted in **Figure 2**. We observed that, the temperature declined with higher enhanced values. Physically, the Slip factor is proportional to the dynamic viscosity. The dynamic viscosity improves temperature on SS. **Figure. 3** illustrate that the N_t (Thermophoresis) on $\theta(\eta)$ with escalating statistical values of N_t. From this figure, we can observe that the temperature is enhanced with distinct ascending values of N_t. Physically, the N_t is inversely proportional to υ^* ("Thermal Diffusivity"). The large of N_t means high υ^*, which is related to motion of flow in porous medium, and it is produce resistance force to liquid motion. Due to this fact the both temperature and concentration reduces when ascending values of N_t. **Figure 4** exhibited the important of N_t (Brownian Motion Parameter) on $\phi(\eta)$. We can see that, the concentration declined numerical values of N_t. Physically, the N_t is proportional to solid particle heat capacity and liquid capacity. The higher values of N_t, high heat capacity of fluid motion. Due to this it is produce concentration decreases and related boundary layer thickness is reducing. The impact of γ (Chemical reaction Parameter) on $\phi(\eta)$ with large values of γ as depicted in **Figure 5**. We found that declined concentration $\phi(\eta)$ for ascending values of γ. Physically, the γ is inversely proportional to υ^* (Kinematic Viscosity). **Figures 6** presented the significant of Le ("Lewies Number") on Heat Transfer Rate. We noticed that $\theta(\eta)$ enhances with distinct numerical values of Lewies number. Physically, the chemical reaction is proportional to k^* ("Mass Absorption"). **Figure 7(a)-7(b)** illustrated the impact of Pr (Prandtl Number) on $\theta(\eta)$ and mass transfer rate respectively. We can see that the temperature and mass transfer rate enhance with escalating numerical values of Prandtl number.

Conclusion:

The present work main outcomes as below:

- The temperature and mass transfer rate enhances with higher statistical values of Prandtl number
- The heat transfer rate enhances for large numerical values of Lewies number.
- The concentration of nanofluid motion is declined for enhanced values of chemical reaction and Brownian motion parameter.

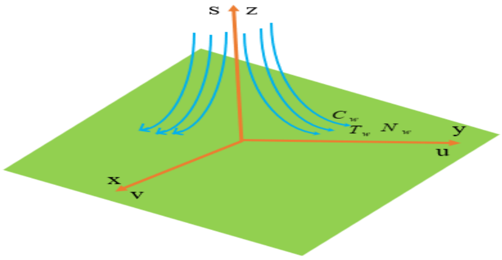

Fig. 1 Physical Model of the Problem

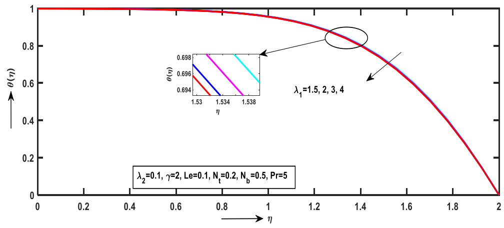

Fig. 2 Influence of λ_1 on $\theta(\eta)$

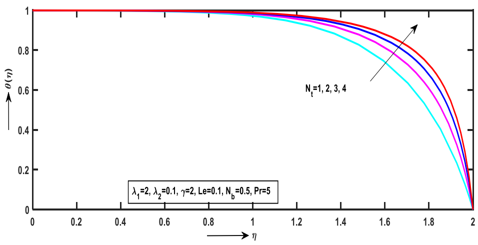

Fig. 3 Influence of N_t on $\theta(\eta)$

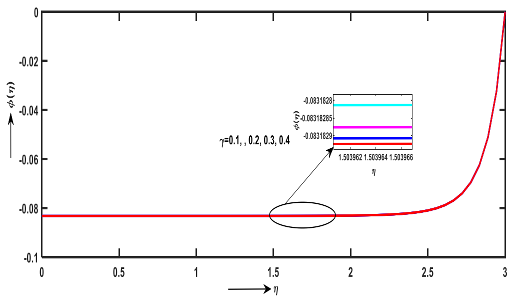

Fig. 5 Influence of γ on $\phi(\eta)$

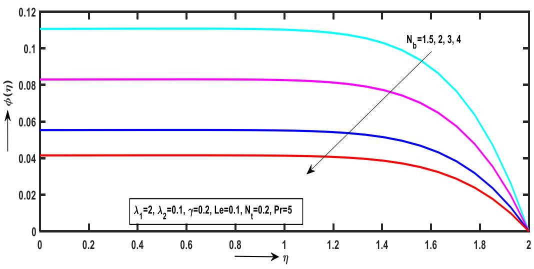

Fig. 4 Influence of N_t on $\phi(\eta)$

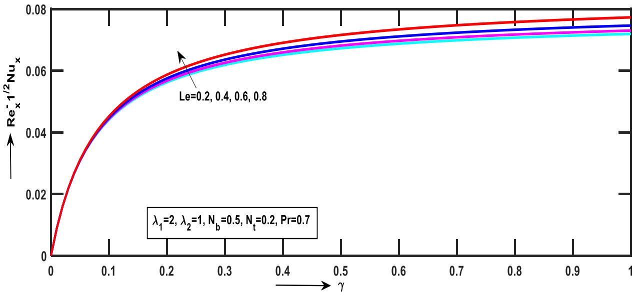

Fig. 6 Influence Le on Heat Transfer Rate

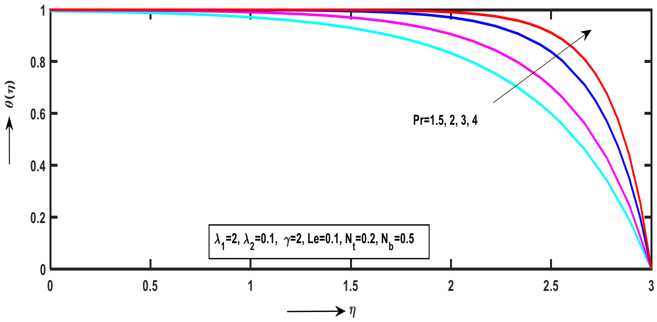

Fig. 7(a) Influence of $\Pr$ on Temperature

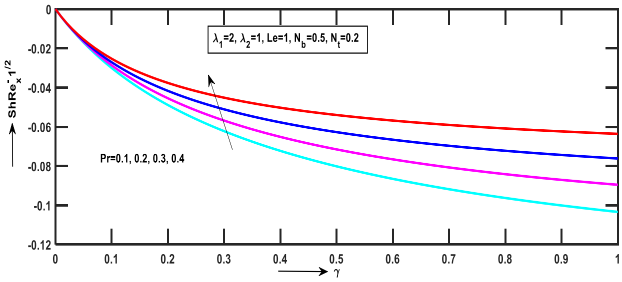

Fig. 7(b) Influence of $\Pr$ on Mass Transfer Rate

References:

1. B. Narsimha Reddy, P. Maddileti and C. Chesneau, Stagnation Point on MHD boundary layer flow of heat and mass transfer over a non-linear stretching sheet with effect of Casson nanofluid, International Journal of Modelling and Simulation, (2023). https://doi.org/10.1080/02286203.2023.2286420.
2. U. Khan, A. Zaib, A. Ishak, I. Waini, I. Pop, S. Elattar and A.M. Abed, Stagnation point flow of a water-based graphene-oxide over a stretching/shrinking sheet under an induced magnetic field with homogeneous-heterogeneous chemical reaction, Journal of Magnetism and Magnetic Materials, 565 (1) (2023) 170287. https://doi.org/10.1016/j.jmmm.2022.170287.
3. Z. Mahmood, F.Z. Duraihem, U. Khan and A.M. Hassan, Model-based comparative analysis of MHD stagnation point flow of hybrid nanofluid over a stretching sheet with suction and viscous dissipation, Numerical Heat Transfer, Part-B: Fundamentals, (2023). https://doi.org/10.1080/10407790.2024.2318457.
4. M. Vinodkumar Reddy, M. Ajithkumar, S.S. Bin Zafar, F. Ali and P. Lakshminarayana, Magnetohydrodynamic stagnation point flow of Williamson hybrid nanofluid via stretching sheet in a porous medium with heat source and chemical reaction, Proceedings of the Institution of Mechanical Engineers, Part E: Journal of Process Mechanical Engineering, (2024). https://doi.org/10.1177/09544089241239583.
5. E.O. Fatunmbi, A.S. Oke and S.O. Salawu, Magnetohydrodynamic micropolar nanofluid flow over a vertically elongating sheet containing gyrotactic microorganisms with temperature-dependent viscosity, Results in Materials, 19 (2023) 100453.

6. M. Boujelbene, A. Majeed, N. Baazaoui, K. Barghout, N. Ijaz, N. Abu-Libden, S. Naeem, I. Khan and M.R. Ali, Effect of electrostatic force and thermal radiation of viscoelastic nanofluid flow with motile microorganisms surrounded by PST and PHF: Bacillus anthracis in biological applications, Case Studies in Thermal Engineering, 52 (2023) 103691.
7. M. Jawad, N. Sadiq and M.R. Ali, Analysis of Chemical Reactive Tangent Hyperbolic Nanofluid Flow with Joule Heating and Motile Microorganisms Through Stretchable Surface, Bio Nanoscience, 14 (2024) 605-618.
8. Y. Li, Y. Leng, N. Baazaoui, M. Bilal Arain, N. Ijaz and A.M. Hassan, Exploring the dynamics of active swimmers microorganisms with electromagnetically conducting stretching through endothermic heat generation/assimilation flow: Observational and computational study, Case Study in Thermal Engineering, 51 (2023) 103560.
9. N. Fatima, A. Majeed, K. Sooppy Nisar, S. Naeem, M.K. Alaoui, N. Saleem and N. Ijaz, Three-dimensional analysis of motile-microorganism and heat transportation of viscoelastic nanofluid with nth order chemical reaction subject to variable thermal conductivity, Case Studies in Thermal Engineering, 45 (2023) 102896.
10. S. Sun, S. Li, S. Shaheen, M. Bilal Arain, Usman and K. Ali Khan, A numerical investigation of bio-convective electrically conducting water-based nanofluid flow on the porous plate with variable wall temperature, Numerical heat Transfer, Part A: Applications, (2023). https://doi.org/10.1080/10407782.2023.2242579.
11. Z. Hussain, W.A. Khan, M. Irfan, H. Shahid, M. Ali, T. Muhammad and M. Waqas, Impact of chemical processes on magnetized tangent hyperbolic nanofluid with bio-convection aspects, Results in Engineering, 20 (2023) 101615.
12. G. Dharmaiah, F. Mebarek-Oudina, J.L. Rama Prasad, Ch. Baby Rani, Exploration of bio-convection for slippery two-phase Maxwell nanofluid past a vertical induced magnetic stretching regime associated for biotechnology and engineering, Journal of Molecular Liquids, 391 (Part B) (2023) 123408.
13. J. Iqbal, F.M Abbasi, M. Alkinidri and H. Alahmadi, Heat and mass transfer analysis for MHD bioconvection peristaltic motion of Powell-Eyring nanofluid with variable thermal characteristics, Case studies in Thermal Engineering, 43 (2023) 102692.
14. M. Naveed Khan, S. Ahmad, Z. Wang, N.A. Ahammad and M.A. Elkotb, Bioconvective surface-catalyzed Casson hybrid nanofluid flow analysis by using thermodynamics heat transfer law on a vertical cone, Tribology International, (188) (2023) 108859.
15. J. Ahmad, F. Nazir, B.M. Fadhl, B.M. Makhdoum, Z. Mahmoud, A. Mohamed and I. Khan, Magneto-bioconvection flow of Casson nanofluid configured by a rotating disk in the presence of gyrotatic microorganisms and Joule heating, Heliyon, 9(8) (2023) e18028.
16. A. Hussain, S. Riaz, A. Hassan, M.Y. Malik, A.S. Alqahtani, H. Karamti, A.M. Saeed, S.M. Eldin, Magneto-Bio-Convection Enhanced heat transfer in Prandtl hybrid nanofluid with inclined magnetization and microorganism migration, Journal of Magnetism and Magnetic Materials, 588 (Part A) (2023) 171403.
17. U. Farooq and L. Tao, Non-similar analysis of MHD bioconvective nanofluid flow on a stretching surface with temperature-dependent viscosity, Numerical Heat Transfer, Part A: Applications, (2023). https://doi.org/10.1080/10407782.2023.2279249.
18. M. Abbas and N. Khan, Numerical study for bioconvection in Marangoni convective flow of Cross nanofluid with convective boundary conditions, Advances in Mechanical Engineering, (2023). https://doi.org/10.1177/168781322312076.
19. A.A.M. Arafa, S.A. Hussein and S.E. Ahmed, Hydrothermal bioconvective Bödewadt ternary composition nanofluids flow over a stretching rotating disk through a heat generating porous medium, Journal of Magnetism and Magnetic Materials, 586 (2023) 171174.
20. I. Ullah, W.A. Khan, W. Jamshed, A.A. Elmonem, N.S. Elmki Abdalla, R.W. Ibrahim, M.E. Eid, F.A. Aziz Elseabee, Heat generation (absorption) in 3D bioconvection flow of Casson nanofluid via a convective heated stretchable surface, Journal of Molcular Liquids, 392(1) (2023) 123503.
21. V. Puneeth, F. Ali, M.R. Khan, M. Shoaib Anwar and N. Ameer Ahammad, Theoretical analysis of the thermal characteristics of Ree-Eyring nanofluid flowing past a stretching sheet due to bioconvection, Biomass Conversion and Biorefinery, (2024) 8649-8660.

22. A. Kumar Sarma, and D. Sarma, Unsteady magnetohydrodynamic bioconvection Casson fluid flow in presence of gyrotactic microorganisms over a vertically stretched sheet, Numerical Heat Transfer Part A: Applications, (2024).
https://doi.org/10.1080/10407782.2024.2389338.
23. Z. Khan, E.N. Thabet, S. Habib, A.M. Abd-Alla, F.S. Bayones, F.M. Alharbi, A.S. Alwabli, Numerical study of hydromagnetic bioconvection flow of micropolar nanofluid past an inclined stretching sheet in a porous medium with gyrotactic microorganism, Journal of Computational Science, 78 (2024) 102256.
24. U. Farooq, Haseena, A. Jan, S.O. Hilali, M. Alhagyan and A. Gargouri, Bioconvection study of MHD hybrid nanofluid flow along a linear stretching sheet with Buoyancy effects: Local Non-Similarity Method, International Journal of Heat and Fluid Flow, 107 (2024) 109350.
25. U. Farooq, T. Liu, U. Farooq and S. Majeed, Non-similar analysis of bioconvection MHD micropolar nanofluid on a stretching sheet with the influences of Soret and Dufour effect, Applied Water Science, 14 (2024).

Nomenclature	
$a_1,\ b_1$ Constants	$\nabla^2 = \partial^2/\partial x^2 + \partial^2/\partial y^2 + \partial^2/\partial z^2$ Laplace Operator
Nu_x Nusselt number	T_f Temperature of hot fluid (K)
u^*, v^*, w^* Velocity components along x_1, y_1, z_1 $(\mathrm{m s^{-1}})$	T_1 Fluid temperature (K)
C_1 Nanoparticle volume fraction (mol/m^3)	T_∞ Ambient fluid temperature
c_p Specific heat constant $(kJ/kg\cdot K)$	U_∞ Free stream velocity $(m s^{-1})$
C_f Skin friction coefficient	U_w, V_w Stretching velocities
C_∞ Uniform ambient concentration (mol/m^3)	W_c Maximum cell swimming speed
C_w Nanoparticle concentration (mol/m^3)	λ_i Slip factors $= N_i\sqrt{a_1\mu^*}$
D_n Diffusivity of microorganisms	λ_1 Slip Length along x- axis
D_B Brownian diffusion	λ_1 Slip Length along y- axis
D_T Thermophoresis diffusion $(m^2.s^{-1})$	***Greek symbols***
f' Dimensionless velocity	α_m Thermal Diffusivity $(m^2.s^{-1})$
f Dimensionless stream function	$(\rho c)_p$ Heat capacity of the nanoparticle $(kJ\ kg^{-1})$
h_f Heat transfer coefficient $(W\,m^{-2}\,K^{-1})$	
k Thermal Conductivity $(W\,m^{-1}\,K^{-1})$	$(\rho c)_f$ Heat capacity of the field $(kJ\ kg^{-1})$
k^* Mean absorption coefficient	ϕ Dimensionless concentration

Le Lewis number $\frac{\alpha_m}{D_B}$	η Similarity variable
N_t Thermophoresis parameter $=\frac{\tau^* D_T (T_w - T_\infty)}{\alpha_m T_\infty}$	μ^* Dynamic viscosity $(N\ s\ m^{-2})$
N_b Brownian motion coefficient $=\frac{\tau^* D_B (C_w - C_\infty)}{\alpha_m}$	θ Dimensionless temperature
$N_1,\ N_2$ Slip coefficients in x and y	ρ_f Fluid density $(k\,g/\,m^3)$
$\Pr$ Prandtl number $=\frac{\upsilon^*}{\alpha_m}$	γ Surface Convection Parameter $\frac{h_f}{k}\left(\sqrt{\upsilon / a}\right)$
p_0 Stagnation pressure	τ^* Ratio of the nanoparticle to fluid $(\rho c)_p / (\rho c)_f$
p Fluid Pressure $kg / m\ .s^2$	υ^* Kinematic viscosity $=\frac{\mu^*}{\rho_f}\ (m^2 s^{-1})$
Pe Bio-convection Peclet number $=\frac{bW_c}{D_n}$	b Chemotaxis Constant
q_m Mass Flux at the wall $(k\,g\,s^{-1}\,m^{-1})$	***Subscripts***
q_w Heat Flux at the wall $(W\,m^{-2})$	∞ condition at free stream
Re_x Reynolds number	W Wall mass transfer velocity $(\mathrm{m\,s}^{-1})$
Sc Schmidt number $=\frac{\upsilon^*}{D_n}$	W_c Maximum Cell Swimming Speed
Abbreviations	
HT Heat Transfer	TC Thermal Conductivity
TR Thermal Radiation	NPs Nanoparticles
NFs Nanofluids	SP Stagnation Point
HTR Heat Transfer Rate	3D Three Dimensional
MHD Magnetohydrodynamic	TR Thermal Radiation
QSS Quasi Steady State	HMT Heat and Mass Transfer
AS Anisotropic Slip	BC Boundary Condition
BL Boundary Layer	PM Porous Medium
WL Williamson Liquid	GM Gyrotatic Microorganisms
WNFs Williamson Nanofluids	HNFs Hybrid Nanofluids
HF Heat Flux	CC Cattaneo- Christov
EG Energy generation	NNFs non-Newtonian Fluids
ASC Anisotropic Slip Condition	